



# Ammonia gas sensors based on polypyrrole films: Influence of electrodeposition parameters

Tilia Patois<sup>a</sup>, Jean-Baptiste Sanchez<sup>b</sup>, Franck Berger<sup>b</sup>, Jean-Yves Rauch<sup>c</sup>, Patrick Fievet<sup>a</sup>, Boris Lakard<sup>a,\*</sup>

<sup>a</sup> Institut UTINAM, UMR CNRS 6213, University of Franche-Comté, 16 route de Gray, 25030 Besançon Cedex, France

<sup>b</sup> Laboratoire Chrono-Environnement, UMR CNRS 6249, University of Franche-Comté, 16 route de Gray, 25030 Besançon Cedex, France

<sup>c</sup> Institut FEMTO-ST, UMR 6174, CNRS UFC ENSMM UTBM, 32 avenue de l'Observatoire, 25044 Besançon Cedex, France

## ARTICLE INFO

### Article history:

Received 16 February 2012

Received in revised form 26 April 2012

Accepted 1 May 2012

Available online 9 May 2012

### Keywords:

Gas sensors

Conducting polymer

Polypyrrole

Electrochemistry

Ammonia

Morphology

## ABSTRACT

A gas sensor consisting in polypyrrole films electrochemically deposited on microelectrodes arrays was fabricated using silicon microtechnologies. Polypyrrole was electrodeposited on platinum microelectrodes using four different electrodeposition potentials, five counter-ions and three salt concentrations to assess the effects of these parameters on the sensing properties of polypyrrole films. The change in conductance of thin polymer layers, due to adsorption of ammonia gas, was used as a sensor signal. The behaviors of the polymer-based gas sensors, including response time, response amplitude, reproducibility and reversibility, to various ammonia gas concentrations ranging from 1 to 100 ppm were investigated. The experimental results showed that these ammonia gas sensors were efficient since they were sensitive to ammonia, and since their response was fast and reproducible at room temperature. The most efficient ammonia gas sensor was obtained with a 248 nm-thick polypyrrole film electrosynthesized from 0.1 M pyrrole and 0.1 M LiClO<sub>4</sub> under an electrodeposition potential of +2.0 V/SCE.

© 2012 Elsevier B.V. All rights reserved.

## 1. Introduction

Since polyacetylene was first shown to have high electrical conductivities when properly doped [1,2],  $\pi$ -conjugated polymers have been studied extensively, and subsequently, used in various applications such as: field effect transistors [3,4], solar cells [5,6], electrocatalysis [7,8], protection against corrosion [9,10], (bio)sensors [11–13] or cell culture [14–17]. Among the various conducting polymers, polypyrrole (PPy) stays one of the most studied because of its easy deposition from aqueous and non-aqueous media, its adherence to many types of substrates, its high electrical conductivity and its stability in air and aqueous media. The simplicity of preparation and the possibility to control experimental conditions by electrochemical techniques make it the most employed way. Moreover, it is now well-known that many chemical or physical properties of electrodeposited polypyrrole can be strongly varied by modifying the electropolymerization parameters including: solvent [18–21], current density [22], pH [23], temperature [24], pyrrole concentration [25–27], electrodeposition potential [26–28], counter-ion [19,26,27,29–31] and its concentration [32]. Furthermore, it has already been demonstrated that electrochemical polymerization conditions, particularly

counter-ion type, can strongly affect the conductivity of polypyrrole films [27,30]. Indeed, large organic counter-ions induce higher conductivity in PPy films, because they are more efficient space fillers and produce isotropic polymers with higher crystallinity than those incorporating small inorganic species [27,30]. This is of importance since the initial conductivity of the polymer film is supposed to impact on the gas sensitivity of the polymer film to ammonia gas [33]. The morphological features of polypyrrole films also strongly modify their properties. For example, polypyrrole films prepared by Kaynak [32], in solutions with high concentration of *p*-toluenesulfonic acid, exhibited a higher roughness than those elaborated in less concentrated solutions. The nature of the counter-ions can also influence the polypyrrole's film morphology as shown by Fang et al. [34]. Indeed, they observed that the use of different counter-ions led to polymer films with very different roughness and morphology. Furthermore, both roughness and morphology of the films greatly influenced the response of the polypyrrole films to ethanol vapor when used as sensor's sensitive layer. Our research group has also studied the effect of counter-ion's type, pyrrole concentration and electrodeposition potential on the conductivity [27] and morphological features of polypyrrole films [26]. Concerning the conductivity [27], it was shown that: (i) increasing the pyrrole concentration increased the film conductivity, (ii) the highest conductivity was obtained for an electrodeposition potential similar to pyrrole oxidation peak's, (iii) biggest counter-ions, such as *p*-toluenesulfonate or

\* Corresponding author.

E-mail address: [boris.lakard@univ-fcomte.fr](mailto:boris.lakard@univ-fcomte.fr) (B. Lakard).

1-naphthalenesulfonate, led to the highest conductivity. Concerning the morphological features [26], the roughness of the films was proved to be very dependent on the counter-ion type since the biggest anions led to very flat surfaces having a small roughness and a high homogeneity. On the contrary, the smallest anions tested or the use of a high electrodeposition potential led to high roughness. Since the electropolymerization conditions strongly influence the properties of polypyrrole films, it can be supposed that they also influence the gas detection efficiency of the polymer films, even if the influence of polymerization parameters on the gas detection efficiency of conducting polymer-based sensors has received little attention in the literature until now.

In this context, the present work aims at investigating the influence of the electropolymerization parameters on the gas detection efficiency of polypyrrole-based sensors and at studying the correlation between conductivity or morphological features of the polypyrrole films and their gas detection efficiency. That is why polypyrrole films were electropolymerized at electrodeposition potentials varying from +0.7 to +2.0 V/SCE, with 5 counter-ions of different sizes: *p*-toluenesulfonate ( $\text{TsO}^-$ ), naphthalenesulfonate ( $\text{NS}^-$ ), nitrate, tetrafluoroborate, and perchlorate anions, and at salt concentration varying from 0.01 to 0.5 M. These various polypyrrole films were electrodeposited on microsystems fabricated using silicon microtechnology. The so-obtained gas sensors consisted of platinum microstructured electrode arrays. The polymer films were deposited on these microelectrodes and also across the insulating gap separating the microelectrodes of the sensor since the insulating gap between the neighboring electrodes was close enough, around  $4\ \mu\text{m}$ , to allow the polymer film to coat the insulated gap and to connect microelectrodes. Then, these polypyrrole-based chemiresistors were tested for ammonia gas sensing. In particular, their response, in terms of conductance changes when exposed to different ammonia concentration, was studied.

## 2. Experimental

### 2.1. Microsystems fabrication

The elaboration of the gas sensors began with the microsystems fabrication using lift-off process that consists in a photolithography followed by a cathodic sputtering to obtain platinum patterns deposited on 4" silicon wafers. To make the desired pattern, consisted of two interdigitated microelectrodes combs, it was necessary to fabricate a Cr/Glass mask for lithography. This mask was designed using Cadence conception software, and it was fabricated using a Heidelberg DWL 250 optical pattern generator. Silicon wafers used in this study were 100-oriented,  $500\ \mu\text{m}$  thick, *p*-type doped and had a resistivity of  $1\text{--}10\ \Omega\ \text{cm}^{-1}$ . They were thermally wet-oxidized, at  $1200\ ^\circ\text{C}$  in water vapor flux during 12 h, in order to produce a  $1.4\ \mu\text{m}$  thick  $\text{SiO}_2$  layer. Wafers and mask were pre-cleaned with a solution containing 50 mL of  $\text{H}_2\text{SO}_4$  and 30 mL of  $\text{H}_2\text{O}_2$ . This step was necessary to remove organic residues at the surface in order to start process in better conditions. Then, the wafer was dried and placed on a hot plate (Prazitherm) for 10 min at  $120\ ^\circ\text{C}$ . Next, a layer of negative photoresist (AZ 5214, from Clariant) was deposited by spin-coating thanks to an RC8-Karlsuss spin coater (30 s at a rotation speed of 3000 rpm). Wafer was again placed on the hot plate for 150 s at  $120\ ^\circ\text{C}$ , before the photoresist was exposed, with the mask at the right position after alignment, to an UV radiation flux of  $36\ \text{mJ}\ \text{cm}^{-2}$  delivered by a double-sided EVG 620 aligner. After 2 min at  $120\ ^\circ\text{C}$  on the hot plate, the wafer was exposed, without the mask, to an additional UV dose of  $210\ \text{mJ}\ \text{cm}^{-2}$ . Therefore, the pattern drawn on the mask was transferred to the resist, which was then developed, by

immersion in AZ 726 developer for 1 min, to reveal the pattern. At the end of the negative photolithography process, optical microscopy was used to ensure the correct development of the resist, and a Fogale-Microsurf 3D profilometer was used to control the thickness of the deposited layer ( $1.4\ \mu\text{m}$ ). Then, with magnetron sputtering Plassys MP 500 system, it was possible to realize the electrode layer. The vacuum chamber was first pumped down to  $3 \times 10^{-6}$  mbar with primary rotating oil pump and secondary cryogenic CT18 pump. Before the depositing step, and in order to increase the adhesion of the layer, 1 min of etching run at a pressure of  $7 \times 10^{-3}$  mbar with argon gas and 250 W of RF power was performed. Then, a thin adhesion of pure titanium layer (30 nm) was sputtered to improve the adhesion of the platinum layer. The deposition of a pure platinum layer (150 nm) was then achieved to realize the electrode system of the sensors. Sputtering deposition parameters were as follows: sputtering pressure (Ar):  $7 \times 10^{-3}$  mbar, power: 150 W with DC Huttinger generator, deposition time: 15 s at 1 A for the Ti layer and 1 min at 0.6 A for the Pt layer. The last step was the dissolution of the remaining resist in acetone with ultrasonic bath. The final optical control was done to eliminate microsystems containing some defects. The sensor geometry, consisting of two interdigitated microelectrodes combs (Fig. 1a), was chosen because it allows to measure conductivity changes between the 2 combs, optimizes the signal delivered by the sensor, and allows the electrodeposition of the polymer both on the combs and in the gap between the 2 combs. Each microelectrode comb was composed of 50 bands measuring  $100\ \mu\text{m}$  wide and  $9996\ \mu\text{m}$  long. The gap between the two combs was  $4\ \mu\text{m}$  so that the polymer can be deposited in this gap and can inter-connect the two combs (Fig. 1b and c).

### 2.2. Electrochemistry

Electropolymerization of polypyrrole films was performed with a PGZ 100 potentiostat (Tacussel-Radiometer Analytical SA-France) controlled by using the VoltaMaster 4 software. A standard three-electrode electrochemical set-up was used. The reference electrode was a Saturated Calomel Electrode (SCE) and the counter-electrode was a platinum sheet. The working electrode was the platinum combs of the microsystem. All electrochemical experiments were carried out at room temperature (293 K). Pyrrole was from ACROS (article 15771 1000, 99% pure) and was distilled under reduced pressure before use. All salts were from Sigma Aldrich and were used as received: lithium perchlorate ( $\text{LiClO}_4$ ), sodium nitrate ( $\text{NaNO}_3$ ), sodium *p*-toluenesulfonate ( $\text{NaTsO}$ ), sodium tetrafluoroborate ( $\text{NaBF}_4$ ), sodium perchlorate ( $\text{NaClO}_4$ ) and sodium naphthalenesulfonate ( $\text{NaNS}$ ). Chronocoulometry was used in order to coat all platinum combs with a polypyrrole film of  $\sim 250\ \text{nm}$ . Thus an electrodeposition potential of +1 V/SCE was applied until reaching a total electric charge density of  $99.2\ \text{mC}\ \text{cm}^{-2}$ , corresponding to a polypyrrole thickness of 248 nm, according to the Faraday's law [26,27]. However, since the charge efficiency of the pyrrole electropolymerization could be different at various electrodeposition potentials, the polymer film thickness could be slightly different even if the total electric charge density was the same for all experiments. Furthermore, Faraday's law was used to determine polypyrrole film thickness rather than measurements performed by optical profilometry or by SEM because Faraday's law allowed obtaining the average thickness of the polymer films when profilometry led only to local measurements of the thickness even if it gave additional information about the sample roughness.

Glucose Discharge Optical Emission Spectrometry measurements were done to confirm the presence of dopants inside the polypyrrole film or/and on its surface using a GD Profiler HORIBA Jobin Yvon.

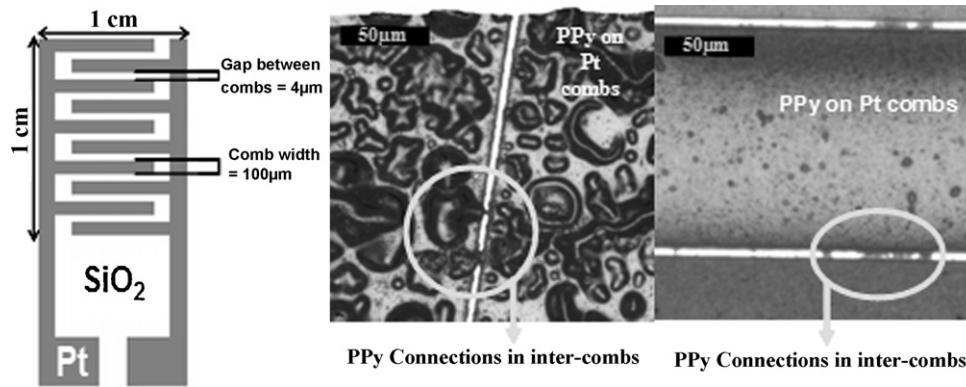


Fig. 1. Schematic drawing of the microsystem (a), optical microscopy pictures of PPy films deposited on the combs by oxidation of pyrrole doped with  $\text{ClO}_4^-$  (b) or  $\text{TsO}^-$  (c).

### 2.3. Gas chamber

All experiments were performed under the same conditions using the experimental set-up described in Fig. 2. At first, each sensor was exposed for 1 h to a purified air flow of  $50 \text{ mL min}^{-1}$  in order to stabilize the sensor and its electrical response in a controlled environment. Indeed, air does not react with PPy layer and a complete stabilization of the baseline was observed after 30 min. The value of conductance measured after this stabilization was considered to be the initial conductance, denoted  $G_0$ . This synthetic air was used, as carrier gas, for both stabilization and dilutions. Then, the sensors were exposed for 5 min to ammonia, initially concentrated at 100 ppm. Each sensor's electrical response was obtained under a constant gas flow (synthetic air or  $\text{NH}_3$  diluted in the synthetic air) rate of  $50 \text{ mL min}^{-1}$ . Mass flowmeters were used to obtain different  $\text{NH}_3$  concentrations (varying from 1 to 100 ppm). This experimental set-up allowed PPy-based gas sensors to be exposed at different ammonia concentrations. Between each exposition to ammonia, the sensors were exposed to synthetic air during 1 h to allow desorption of ammonia molecules from the sensors.

### 2.4. Gas measurements

Real-time monitoring of the sensor's responses was obtained by measuring the evolution of the electrical potential with time (a measurement was made every 2 s). This was done using a data acquisition system, including a multi channel inputs allowing simultaneous connection of up to 4 sensors. The system was interfaced by a computer and data were obtained using Labview. As indicated in the experimental set-up, the sensor's electrical potential was recorded using a divisor voltage bridge (Fig. 2). Under these experimental conditions, the relationship between the voltage  $U_r$  and the sensor's conductance  $G$ , can be expressed by:

$$G = \frac{1}{R((E/U_r) - 1)}$$

where  $E = 5 \text{ V}$  is the terminal voltage applied in the circuit and maintained constant during the experiments and  $R$  the adjusted resistance.

Then,  $G$  was divided by  $G_0$  corresponding to the stabilized conductance under air flow before exposition of the sensor to ammonia gas. The temperature of the sensitive layer during the gas measurements was close to room temperature.

## 3. Results and discussion

### 3.1. Electrochemical synthesis of polymer films

Polypyrrole was electrochemically synthesized for the first time in 1979 by Diaz et al. [35]. Subsequently, it has been shown that it can be deposited either by potentiodynamic or potentiostatic method but also that the properties of the polypyrrole films are strongly affected by electropolymerization parameters including electrodeposition potential, pyrrole concentration or supporting salt.

Since one of the important objectives of this work is to correlate the electrochemical conditions used to deposit PPy films with their gas sensing properties, it was decided to use chronocoulometry to electrosynthesize polypyrrole films having the same thickness. Indeed, chronocoulometry consists in applying a constant potential until reaching a fixed electrical quantity of charge, the charge quantity being proportional to the thickness through Faraday's law. Consequently, by using chronocoulometry, it was possible to obtain polypyrrole films all having the same thickness (248 nm) irrespective of the electrodeposition parameters used. The electrodeposition parameters used in this study were: the electrodeposition potential (varying from +0.7 V to +2.0 V/SCE), the salt concentration (varying from 0.01 to  $0.5 \text{ mol L}^{-1}$ ), and the nature of the salt anion since we have already extensively studied the influence of these parameters on the conductivity [27] and morphological features [26] of electrodeposited polypyrrole films [27]. Fig. 3 represents the chronocoulometries obtained during the electro-synthesis, at different electrodeposition potentials, of polypyrrole films in aqueous solutions composed of 0.1 M pyrrole and 0.1 M  $\text{LiClO}_4$ . This figure shows that the kinetics of the polymer growth is strongly influenced by the electrodeposition potential since the time necessary to reach  $99.2 \text{ mC cm}^{-2}$  is very different for each applied electrodeposition potential. For example, the electrodeposition of the 248 nm thick PPy film was performed (from an aqueous solution of 0.1 M pyrrole and 0.1 M  $\text{LiClO}_4$ ) in 14 s for an applied potential of +2.0 V/SCE when it was performed in 149 s for an electrodeposition potential of +0.7 V/SCE. Similarly, an increase of the salt concentration led to a faster electrodeposition of polypyrrole films: 133 s for 0.01 M  $\text{LiClO}_4$ , 47 s for 0.1 M  $\text{LiClO}_4$  and 35 s for 0.5 M  $\text{LiClO}_4$  (in an aqueous solution of 0.1 M pyrrole and with an electrodeposition potential of +1.0 V/SCE). The differences between the electrodeposition times were less important when the counterion was changed (in an aqueous solution of 0.1 M pyrrole and with an electrodeposition potential of +1.0 V/SCE). The fastest electrodeposition time was obtained for  $\text{ClO}_4^-$  anions (47 s for  $\text{LiClO}_4$  and 46 s for  $\text{NaClO}_4$ ) but no general trend was observed as a function of the

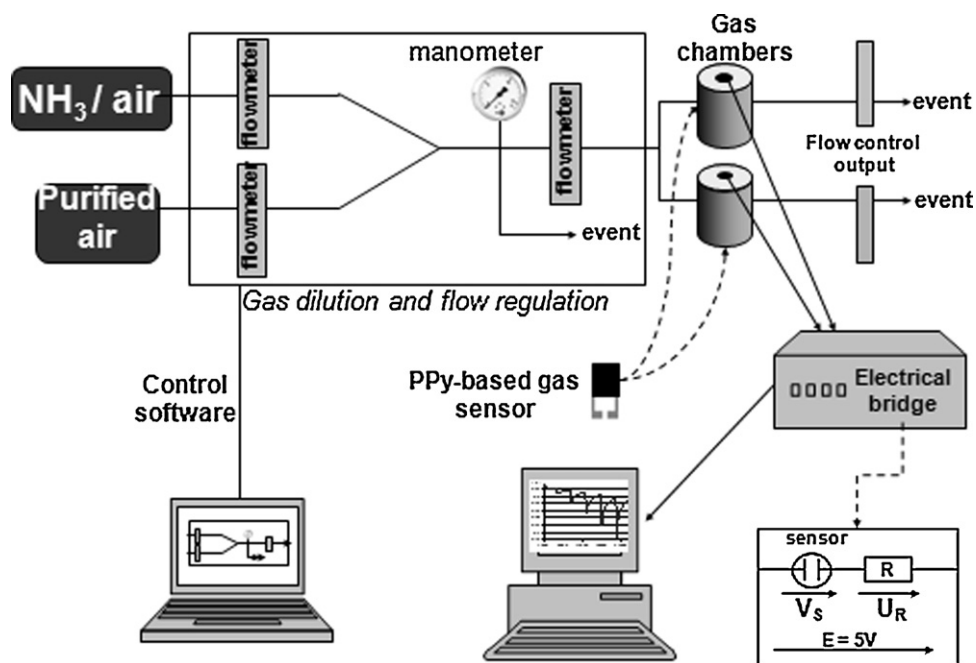


Fig. 2. Experimental set-up for the detection and the analysis of ammonia gas.

anion's size since the electrodeposition times were: 58 s for  $\text{NO}_3^-$ , 88 s for  $\text{NS}^-$ , 93 s for  $\text{TsO}^-$  and 97 s for  $\text{BF}_4^-$ . Furthermore, it must be noticed that the presence of the counter-ion was demonstrated by Glow Discharge Optical Emission Spectrometry measurements. Indeed, this technique allowed us to confirm the presence of Cl element inside the polypyrrole film but also on the surface of the polypyrrole film thus demonstrating that the dopants are present in the polymer film even if the quantification of the dopants in the film is not possible.

### 3.2. Evaluation of the sensor's conductance under ammonia flow

Firstly, the sensor was exposed to synthetic air for stabilization of the baseline, leading to a constant electrical response, and so, to a

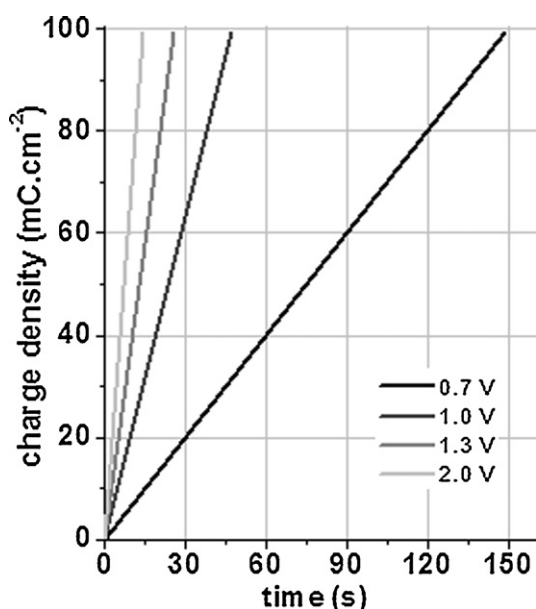


Fig. 3. Chronocoulometry curves obtained during PPy polymerization for electrodeposition potentials varying from +0.7 to +2.0V/SCE.

constant initial conductance  $G_0$ . Then, during 300 s, the sensor was exposed to the ammonia flow, the ammonia being concentrated at 10–100 ppm. This exposition led to a decrease in the sensor's conductance  $G$ , as shown in Fig. 4 that represents the evolution of  $G/G_0$  versus time. After being exposed to ammonia for 300 s, the sensor was again exposed to synthetic air during 3000 s to evaluate its reversibility. The increase of the sensor's conductance observed under exposition to synthetic air, corresponds to desorption of ammonia molecules from the polypyrrole film.

The mechanism of interaction between polymer films and ammonia has already been studied by Carquigny et al. [36] and by Lähdesmäki et al. [37]. Since polypyrrole can be considered as a p-type semi-conducting material composed of both neutral and oxidized monomer units, the ammonia adsorption onto the PPy films was shown to begin with the lost of an electron by the nitrogen's doublet of some nitrogen atoms of the polymer backbone, leading to the formation of  $\text{NH}^+$  radical groups. This electron transfer between ammonia molecule and the polymer's positive hole induces a diminution of the positive charge density which leads to a decrease in the conductance. Consequently, after adsorption of  $\text{NH}_3$ , the polymer becomes less conducting, and the measured conductance decreases. On the contrary, during desorption of the ammonia molecules, the sensor's conductance increases.

### 3.3. Influence of electrodeposition parameters on the sensor's responses

The sensor's responses measured during the exposition of polypyrrole-based gas sensors to ammonia, concentrated at 40 and 75 ppm, are gathered in Table 1. The electrodeposition conditions leading to unexploitable responses are not given in the table but they will be discussed afterwards in the paper. The behavior of the gas sensors was estimated using both the normalized conductance changes ( $100\Delta G/G_0$ ), and the measured slopes of the curves giving the evolution of  $G/G_0$  with time. Indeed, looking at the beginning of the exposition to ammonia flow,  $G/G_0$  variation was linear with time. Consequently, the calculation of the



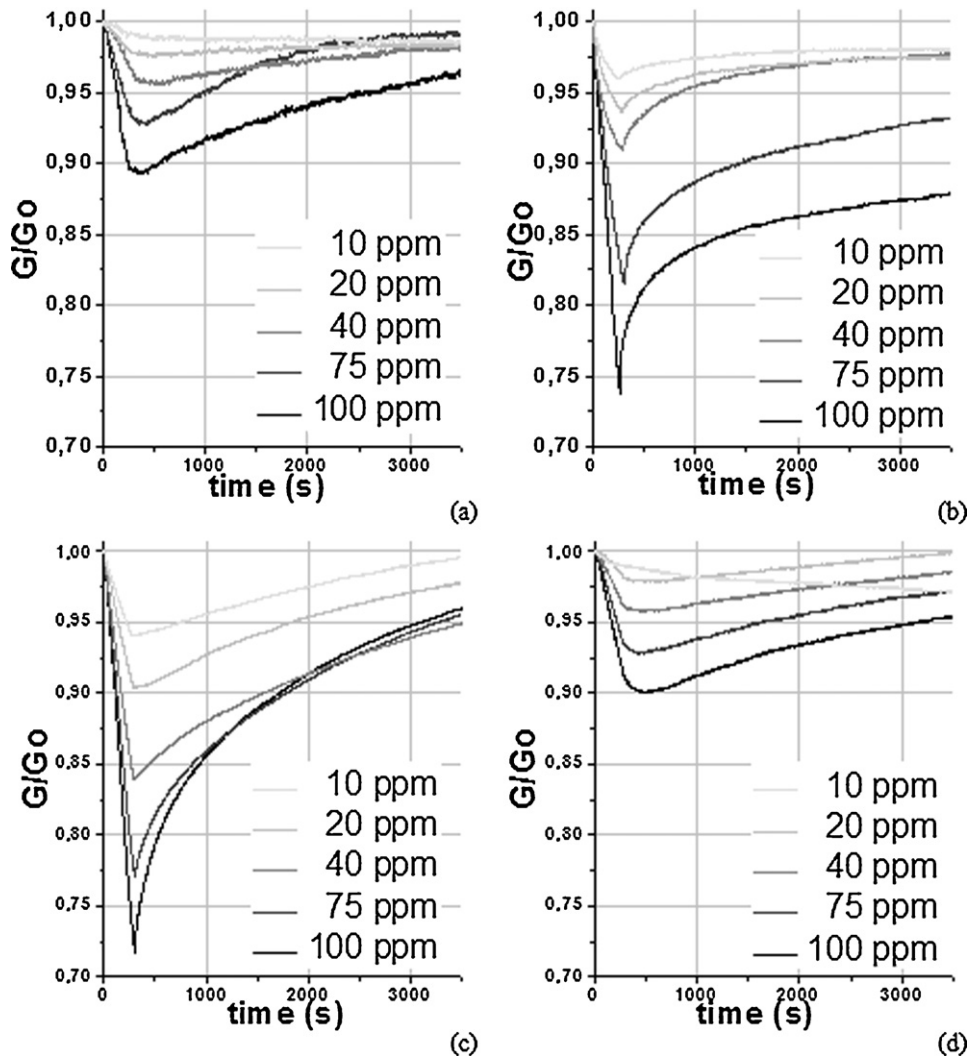


**Fig. 4.** Evolution of the normalized conductance versus time for PPy-based sensors electrodeposited with 0.1 M  $\text{ClO}_4^-$  at  $E_{\text{EDP}} = +1.0$  (a),  $+1.3$  (b),  $+2.0$  V/SCE (c), or with 0.1 M  $\text{NO}_3^-$  at  $+1.0$  V/SCE.

slope values gave us information about the sensitivity of the gas sensor.

### 3.3.1. Influence of the electrodeposition potential on the sensor's responses

Gas sensors were obtained by electropolymerization from an aqueous solution of 0.1 M pyrrole and 0.1 M  $\text{LiClO}_4$  at different electrodeposition potentials ( $E_{\text{EDP}}$ ):  $+0.7$ ,  $+1.0$ ,  $+1.3$  and  $+2.0$  V/SCE. It appears that the sensitivity of the sensors increases with the electrodeposition potential. For example, for gas sensors exposed 300 s to  $\text{NH}_3$  at 75 ppm, the normalized conductance changes were comprised between 0.21% (for  $E_{\text{EDP}} = +0.7$  V/SCE) and 22.8% (for  $E_{\text{EDP}} = +2.0$  V/SCE). Similarly, the slopes of sensor's responses amounted to between  $16.0 \text{ nS s}^{-1}$  and  $1283.0 \text{ nS s}^{-1}$ . Consequently, the increase of the slopes with the electrodeposition potential demonstrates that the polypyrrole-based sensors are most sensitive when the polypyrrole film is electrosynthesized at high electrodeposition potential. Concerning the reversibility, Fig. 4 shows that it is not complete for all sensors and all concentrations but no general trend was observed that might correlate the reversibility with the electropolymerization conditions. For example, the reversibility was good for polypyrrole films obtained at  $+1.0$  V/SCE (only the signal measured for 100 ppm ammonia was not

completely reversible), but was quite unsatisfactory for polypyrrole films synthesized at  $+1.3$  V/SCE. The reversibility could probably be improved by heating the sensors to desorb the ammonia molecules from the polymer films, by using a longer desorption time or by decreasing the exposure time. Indeed, the time of exposure chosen in this work was 300 s, and led to a better reversibility than the one obtained in our previous study in which the exposure time was 6000 s [36].

In another previous work [28], we showed that an increase of the electrodeposition potential led to a decrease in the polymer film's conductivity (from 20,000 to  $600 \text{ S m}^{-1}$ ) since a high electrodeposition potential caused an overoxidation of the polymer leading to C=O bonds that break the conjugation in the heterocyclic polypyrrole. It is possible to propose an explanation to the fact that polymer films having a higher initial conductivity leads to less sensitive gas sensors. Indeed, the adsorption of a given amount of ammonia molecules will only slightly modify the conductivity of a polymer material having a very high conductivity (for example metals). On the contrary, the same amount of ammonia molecules will greatly perturb the conductivity of a semi-conducting material, such as heterocyclic polymer films, having a lower conductivity. The same trend was already reported by Subramanian. In the case of polyaniline-based chemiresistors, they found that the relative

**Table 1**  
Sensor's responses to ammonia changes for different electrodeposition conditions.

Electrodeposition potential (V/SCE)	Electrolyte salt	[NH <sub>3</sub> ] (ppm)	100 ( $\Delta G/G_0$ ) (%)	Slope (nS s <sup>-1</sup> )	
0.7	LiClO <sub>4</sub> (0.1 M)	40	0.17	12.8	
		75	0.21	16.0	
40		3.8	153.2		
75		6.8	310.6		
1.0		40	8.8	622.3	
		75	18.4	1250.0	
1.3		40	16.0	613.9	
		75	22.8	1283.0	
2.0		NaClO <sub>4</sub> (0.1 M)	40	1.0	51.9
			75	1.7	88.3
1.0	NaNO <sub>3</sub> (0.1 M)	40	3.9	314.9	
		75	6.7	464.3	
	NaBF <sub>4</sub> (0.1 M)	40	0.2	86.0	
		75	0.4	166.1	
	LiClO <sub>4</sub> (0.01 M)	40	0.8	73.0	
		75	1.0	88.1	
LiClO <sub>4</sub> (0.5 M)	40	0.2	20.0		
	75	0.3	23.2		

change in conductance decreased with the increase of original conductance [38].

### 3.3.2. Influence of the counter-ion type on the sensor's responses

Gas sensors were obtained by electropolymerization from an aqueous solution of 0.1 M pyrrole at an electrodeposition potential of +1.0 V/SCE. A salt was added, at a concentration of 0.1 M, to this solution. Salts were NaClO<sub>4</sub>, LiClO<sub>4</sub>, NaNO<sub>3</sub>, NaBF<sub>4</sub>, NaTsO or NaNS.

When polypyrrole electropolymerization was performed in an electrolytic solution containing TsO<sup>-</sup> or NS<sup>-</sup> as counter-ions, polymer films exhibited a poor response to ammonia. Since these polymer films possessed the highest conductivities,  $3 \times 10^5$  S cm<sup>-1</sup> and  $1 \times 10^5$  S cm<sup>-1</sup> for TsO<sup>-</sup> and NS<sup>-</sup>, respectively [27], their lack of sensitivity to ammonia demonstrates that the initial conductivity of the polypyrrole films can impact on their gas sensing. The morphology of TsO<sup>-</sup> and NS<sup>-</sup>-doped polypyrrole films can also offer another explanation. Indeed, big anions led to very small values of roughness parameters showing that the polymer samples were flat and homogeneous, whereas polymer films containing small anions led to coatings with higher roughness values [26]. Consequently, the gas sensing may be improved by an increase in the polymer surface roughness.

Other polypyrrole films were doped with counter-anions having a similar size. However, their responses to ammonia were different. Thus, NaNO<sub>3</sub> and LiClO<sub>4</sub> salts leads to the best sensitivities since the normalized conductance changes to 75 ppm ammonia were of 6.7% and 6.8%, respectively. On the contrary, NaBF<sub>4</sub> and NaClO<sub>4</sub> lead to a poor sensitivity of 0.4% and 1.7%, respectively. The response time of the gas sensors to 75 ppm ammonia exhibits the same trend since NaNO<sub>3</sub> and LiClO<sub>4</sub> lead to the fastest responses (464.3 and 310.6 nS s<sup>-1</sup>, respectively) when NaBF<sub>4</sub> and NaClO<sub>4</sub> lead to the slowest responses (166.1 and 88.3 nS s<sup>-1</sup>, respectively).

### 3.3.3. Influence of the salt concentration on the sensor's responses

The responses to ammonia of sensors incorporating polypyrrole films electrosynthesized from 0.01 M and 0.5 M LiClO<sub>4</sub> were also measured and compared to the response obtained from polypyrrole electrosynthesized from 0.1 M pyrrole. The electrodeposition potential was +1.0 V/SCE. Changing the concentration of LiClO<sub>4</sub> in the electrolyte solution does not improve the sensitivity of the sensors (Table 1). Indeed, in the case of polypyrrole films synthesized with 0.01 M LiClO<sub>4</sub>, the sensor's signal was very low since the normalized conductance changes to 75 ppm ammonia was only 1.0%. The morphology of the films obtained at 0.01 M and 0.1 M LiClO<sub>4</sub> being very similar, the poor sensitivity of this sensor may be due to the very low conductivity of the PPy film

( $\sigma_{298K} = 1.1 \times 10^3$  S m<sup>-1</sup>) compared to the conductivity of PPy film obtained from 0.1 M LiClO<sub>4</sub> ( $\sigma_{298K} = 1.3 \times 10^4$  S m<sup>-1</sup>). Indeed, in the case of 0.01 M LiClO<sub>4</sub>, the conductivity is very low and consequently there are very few monomer units in the polymer film that can be reduced by ammonia molecules to generate a conductance signal of the gas sensor. In the case of sensors incorporating PPy films obtained with 0.5 M LiClO<sub>4</sub>, the sensor's signal was also very small. This cannot be due to the conductivity of this polymer film since it is similar to the conductivity of the film obtained from 0.1 M LiClO<sub>4</sub>, thus it may be explained by the morphology of the polymer films since 0.5 M LiClO<sub>4</sub> led to coatings having a very small developed area compared to the other ones [27]. Consequently, the polymer film area allowing the adsorption and diffusion of ammonia molecules was reduced and did not allow to obtaining satisfactory gas measurements.

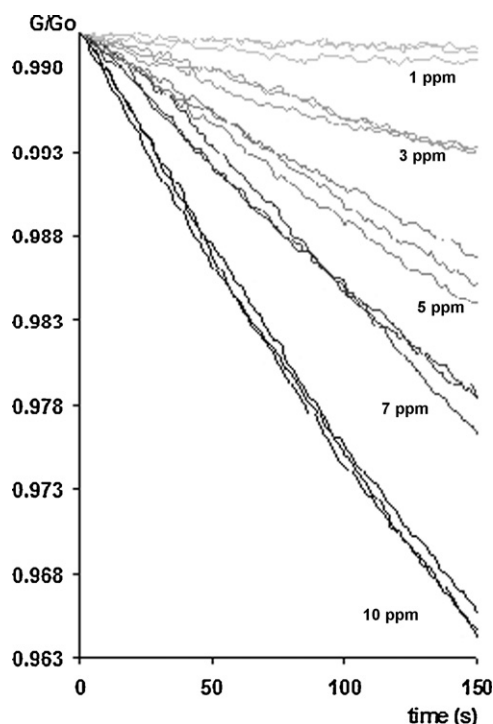


**Fig. 5.** Evolution of the normalized conductance versus time for three different polypyrrole-based sensors (for ammonia concentrations varying from 1 to 10 ppm). PPy films were synthesized from 0.1 M ClO<sub>4</sub><sup>-</sup>, 0.1 M Py,  $E_{EDP} = +2$  V/SCE.

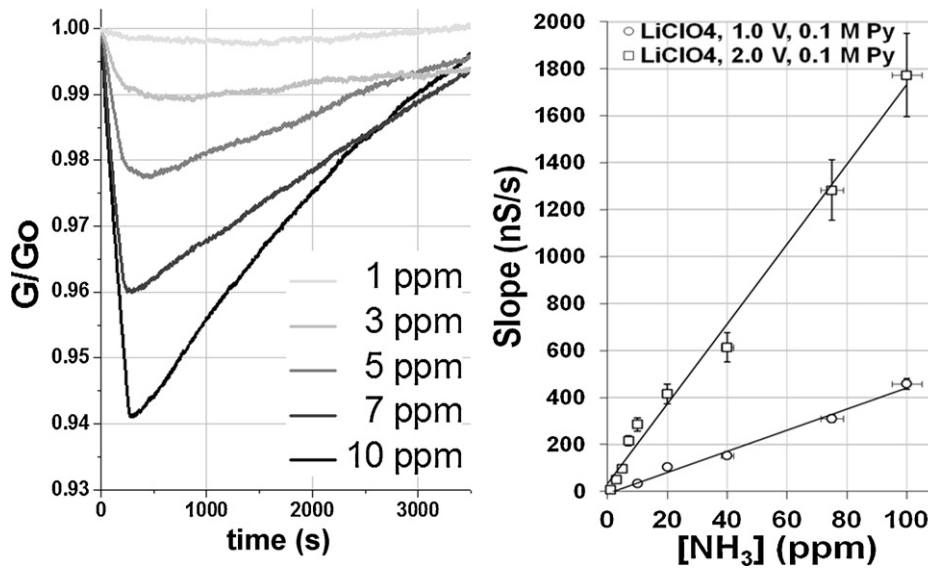


**Fig. 6.** (a) Evolution of polypyrrole-based sensor's normalized conductance versus time for low concentrations of ammonia gas (1–10 ppm) for a polypyrrole film synthesized with 0.1 M  $ClO_4^-$ , 0.1 M Py,  $E_{EDP} = +2.0$  V/SCE and (b) evolution of the slopes of gas sensor's electrical responses to ammonia concentrations.

#### 3.4. Optimization of the PPy-based ammonia gas sensor

From our point of view, an efficient polypyrrole-based gas sensor is characterized by a good sensibility to ammonia concentration, a good reproducibility and a fast response. Consequently, the polymer layer leading to the highest normalized conductance changes and to the highest slope of the curve giving the normalized conductance as a function of time, was chosen for additional investigation. Thus, from the gas measurements previously performed, it appeared that polypyrrole films electrosynthesized from 0.1 M pyrrole, 0.1 M  $LiClO_4$  under an electrodeposition potential of +2.0 V/SCE were the most sensitive. Indeed, this coating leads to very competitive normalized conductance changes: 16.0% when exposed to 40 ppm ammonia and 22.8% when exposed to 75 ppm ammonia (Table 1). Furthermore, the slopes were also the highest ( $1283 \text{ nS s}^{-1}$  when exposed to 75 ppm ammonia), indicating that the sensitivity is optimal in these conditions. The reproducibility of the sensor's response was also quite good as proved by Fig. 5 representing the electrical responses of different sensors, having the same thickness and prepared with the same electropolymerization conditions, to ammonia changes (during the first 150 s of the exposition to ammonia).

The response of this gas sensor was studied more thoroughly, in particular the gas response to more diluted ammonia was measured. Fig. 6a exhibits the polymer-based sensor's response to ammonia at a concentration of 1–10 ppm. Once again, the signal generated by the gas sensor to ammonia gas consisted in a conductance decrease due to the reduction of oxidized units of the polymer backbone. These measurements also show that the limit of detection of the PPy sensor was around 3 ppm (the signal obtained for 1 ppm ammonia was not enough satisfactory to consider 1 ppm as the detection limit). Furthermore, as can be seen in Figs. 4–6, the conductance decrease depends on the concentrations of the pollutant in the gas chamber. In particular, it was possible to determine the slope value of the sensor's response obtained for each ammonia concentration, then to plot the variation of the slopes versus ammonia concentration. Fig. 6b represents the evolution of the slope versus ammonia concentration. A linear relationship was observed between the slope and the ammonia concentration on the whole concentration range. It can also be noticed that polymer-based gas sensors operate at room temperature. This is an

important advantage since other chemiresistors, for example those based on metallic oxides, work at high temperatures (about  $450^\circ\text{C}$ ) in order to optimize the electrical response. On the contrary, we have previously shown that polymer-based gas sensors responses were optimal at  $25^\circ\text{C}$  [36].

Consequently, the characteristics of this latter polypyrrole-based gas sensor are very competitive compared to other ammonia gas sensors based on polypyrrole films. For example, an ammonia gas sensor based on Langmuir–Blodgett PPy film was developed but its detection limit was of 100 ppm in ammonia [39]. Bai et al. had electrochemically co-polymerized polypyrrole and sulfonated polyaniline to obtain an ammonia sensor that was efficient for concentrations higher than 20 ppm [40]. Concerning ammonia sensors based on electrosynthesized PPy film, the most interesting study was conducted by from Brie et al. [33]. This work was done with various doping agents but was limited to concentrations higher than 10 ppm.

#### 4. Conclusion

A gas sensor consisting of interdigitated microelectrode combs electrochemically coated by a polypyrrole film was developed. The electrodeposition conditions (electrodeposition potential, anion concentration and nature of the anion doping the polymer film) were varied to obtain polymer films having different properties and to evaluate the influence of each electrodeposition parameter on the ammonia sensing properties of the polymer films. Thus, the electrodeposition conditions were determined and consisted in an electrodeposition potential of +2.0 V/SCE, a pyrrole concentration of 0.1 M and in the use of  $ClO_4^-$  as dopant. Such conditions led to a gas sensor operating at room temperature with a high detection efficiency, a good reproducibility, a fast response, and a low detection limit (around 3 ppm). The characteristics of this latter polypyrrole-based gas sensor are very competitive compared to other ammonia gas sensors based on polypyrrole films [33,37,39,40]. Furthermore, even if the reversibility of the gas sensors can again be improved, the developed gas sensors present an interesting potential for environmental pollution monitoring since the ammonia sensing measurements were successfully performed in air and since the sensors operated at ambient temperature with a

high sensitivity to ammonia, and with a low detection limit (3 ppm) that is below the ammonia toxicity values since the long-term allowed concentration that people may work in is 20 ppm [41]. Finally, even if it was shown that polypyrrole-based sensors are strongly sensitive to ammonia, it must be noticed that the developed gas sensors are not totally selective. Indeed, polypyrrole is a p-type conducting polymer whose doping level and electric conductance strongly decrease when detecting an electro-donating gas, such as ammonia. The same type of reaction occurs when polypyrrole is exposed to other electro-donating gas. On the contrary, a lot of other gas, such as volatile organic compounds (VOCs), or such as CO, that is rather inert to redox at room temperature, cannot interfere with the detection of ammonia by polypyrrole-based sensors.

## Acknowledgments

Tilia Patois was funded, through a PhD grant, by the Franche-Comté Regional Council. The authors acknowledge the MIMENTO Technology Centre in Besançon, for permit them the entry and the free use of the clean room.

## References

- [1] S. Shirakawa, E.J. Louis, A.G. MacDiarmid, C.K. Chiang, A.J. Heeger, Synthesis of electrically conducting organic polymers: halogen derivatives of polyacetylene, *Journal of the Chemical Society, Chemical Communication* 578 (1977).
- [2] H. Shirakawa, The discovery of polyacetylene film: the dawning of an era of conducting polymers, *Angewandte Chemie International Edition* 40 (2001) 2575–2580.
- [3] I.A. Mir, T. Ahuja, D. Kumlar, D. Taguchi, T. Manaka, M. Iwamoto, Carrier injection from polypyrrole coated gold electrodes in pentacene field effect transistors, *Synthetic Metals* 160 (2010) 2116–2120.
- [4] H. Yoon, J. Jang, A field-effect transistor sensor based on polypyrrole nanotubes coupled with heparin for thrombin detection, *Molecular Crystals and Liquid Crystals* 491 (2008) 21–31.
- [5] D. Gendron, M. Leclerc, New conjugated polymers for plastic solar cells, *Energy Environment Science* 4 (2011) 1225–1237.
- [6] A. Facchetti,  $\pi$ -Conjugated polymers for organic electronics and photovoltaic cell applications, *Chemistry of Materials* 23 (2011) 733–758.
- [7] K. Xue, Y. Xu, W. Song, One-step synthesis of 3D dendritic gold@polypyrrole nanocomposites via a simple self-assembly method and their electrocatalysis for H<sub>2</sub>O<sub>2</sub>, *Electrochimica Acta* 60 (2012) 71–77.
- [8] D. Jia, Q. Ren, L. Sheng, F. Li, G. Xie, Y. Miao, Preparation and characterization of multifunctional polypyrrole–Au coated NiO nanocomposites and study of their electrocatalysis toward several important bio-thiols, *Sensors and Actuators B* 160 (2011) 168–173.
- [9] M. Rizzi, M. Trueba, S.P. Trasatti, Polypyrrole films on Al alloys: the role of structural changes on protection performance, *Synthetic Metals* 161 (2011) 23–31.
- [10] M.C. Turhan, M. Weiser, M.S. Killian, B. Leitner, S. Virtanen, Electrochemical polymerization and characterization of polypyrrole on Mg–Al alloy (AZ91D), *Synthetic Metals* 161 (2011) 360–364.
- [11] U. Lange, N.V. Roznyatovskaya, V.M. Mirsky, Conducting polymers in chemical sensors and arrays, *Analytica Chimica Acta* 614 (2008) 1–26.
- [12] D.C. Tiwari, R. Sharma, K.D. Vyas, M. Boopathi, V.V. Singh, P. Pandey, Electrochemical incorporation of copper phthalocyanine in conducting polypyrrole for the sensing of DMMP, *Sensors and Actuators B* 151 (2010) 256–264.
- [13] O. Segut, B. Lakard, G. Herlem, J.Y. Rauch, J.C. Jeannot, L. Robert, B. Fahys, Development of miniaturized pH biosensors based on electrosynthesized polymer films, *Analytica Chimica Acta* 597 (2007) 313–321.
- [14] L. Zhang, W.R. Stauffer, E.P. Jane, P.J. Sarnak, X.T. Cui, Enhanced differentiation of embryonic and neural stem cells to neuronal fates on laminin peptides doped polypyrrole, *Macromolecular Bioscience* 10 (2010) 1456–1464.
- [15] A. Blau, A. Murr, E. Sernagor, P. Medini, G. Iurilli, C. Ziegler, F. Benfenati, Flexible, all-polymer microelectrode arrays for the capture of cardiac and neuronal signals, *Biomaterials* 32 (2011) 1778–1786.
- [16] B. Lakard, L. Ploux, K. Anselme, F. Lallemand, S. Lakard, M. Nardin, J.Y. Hihn, Effects of ultrasounds on the electrochemical synthesis of polypyrrole, application to the adhesion and growth of biological cells, *Bioelectrochemistry* 75 (2009) 148–157.
- [17] S. Lakard, N. Morrand-Villeneuve, E. Lesniewska, B. Lakard, G. Michel, G. Herlem, T. Gharbi, B. Fahys, Synthesis of polymer materials for use as cell culture substrates, *Electrochimica Acta* 53 (2007) 1114–1126.
- [18] T.F. Otero, J. Rodriguez, Role of protons on the electrochemical polymerization of pyrrole from acetonitrile solutions, *Journal of Electroanalytical Chemistry* 379 (1994) 513–516.
- [19] S. Lee, H. Sung, S. Han, W. Paik, Polypyrrole film formation by solution-surface electropolymerization. Influence of solvents and doped anions, *Journal of Physical Chemistry* 98 (1994) 1250–1252.
- [20] E.L. Kupila, J. Kankare, Electropolymerization of pyrrole in aqueous solvent mixtures studied by in situ conductimetry, *Synthetic Metals* 82 (1996) 89–95.
- [21] S. Carquigny, O. Segut, B. Lakard, F. Lallemand, P. Fievet, Effect of electrolyte solvent on the morphology of polypyrrole films: application to the use of polypyrrole in pH sensors, *Synthetic Metals* 158 (2008) 453–461.
- [22] P. Dyreklev, M. Granstrom, O. Inganas, The influence of polymerization rate on conductivity and crystallinity of electropolymerised polypyrrole, *Polymer* 37 (1996) 2609–2613.
- [23] J.L. Martins, M. Bazzouai, T.C. Reis, S.C. Costa, M.C. Nunes, L. Martins, E.A. Bazzouai, The effect of pH on the pyrrole electropolymerization on iron in malate aqueous solutions, *Progress in Organic Coatings* 65 (2009) 62–70.
- [24] W. Liang, J. Lei, C.R. Martin, Effect of synthesis temperature on the structure, doping level and charge-transport properties of polypyrrole, *Synthetic Metals* 52 (1992) 227–239.
- [25] M. Ogamasawara, K. Funahashi, T. Demyra, T. Hagiwara, K. Iwata, Enhancement of electrical conductivity of polypyrrole by stretching, *Synthetic Metals* 14 (1986) 61–69.
- [26] T. Patois, B. Lakard, S. Monney, X. Roizard, P. Fievet, Characterization of the surface properties of polypyrrole films. Influence of the electrodeposition parameters, *Synthetic Metals* 161 (2011) 2498–2505.
- [27] T. Patois, B. Lakard, N. Martin, P. Fievet, Effect of various parameters on the conductivity of free standing electrosynthesized polypyrrole films, *Synthetic Metals* 160 (2010) 2180–2185.
- [28] M. Chmielewski, M. Grzeszczuk, J. Kalenik, A. Kpas-Suwara, Evaluation of the potential dependence of 2D–3D growth rates and structures of polypyrrole films in aqueous solutions of hexafluorates, *Journal of Electroanalytical Chemistry* 647 (2010) 169–180.
- [29] M. Atobe, H. Tsuji, R. Asami, T. Fuchigami, A study on doping–undoping properties of polypyrrole films electropolymerized under ultrasonication, *Journal of the Electrochemical Society* 153 (2006) D10–D13.
- [30] Y. Li, Y. Fan, Doping competition of anions during the electropolymerisation of pyrrole in aqueous solutions, *Synthetic Metals* 79 (1996) 225–227.
- [31] Y. Osada, D.E. De Rossi, *Polymer Sensors and Actuators*, Springer, London, 2000.
- [32] A. Kaynak, Effect of synthesis conditions on the surface morphology of conducting polypyrrole films, *Materials Research Bulletin* 32 (1997) 271–285.
- [33] M. Brie, R. Turcu, C. Neamtu, S. Pruneanu, The effect of initial conductivity and doping anions on gas sensitivity of conducting polypyrrole films to NH<sub>3</sub>, *Sensors and Actuators B* 37 (1996) 119–122.
- [34] Q. Fang, D.G. Chetwynd, J.A. Covington, C.S. Toh, J.W. Gardner, Micro-gas sensor with conducting polymers, *Sensors and Actuators B* 84 (2002) 66–71.
- [35] A.F. Diaz, K.K. Kanazawa, G.P. Gardini, Electrochemical polymerization of pyrrole, *Journal of the Chemical Society, Chemical Communication* (1979) 635–636.
- [36] S. Carquigny, J.B. Sanchez, F. Berger, B. Lakard, F. Lallemand, Ammonia gas sensor based on electrosynthesized polypyrrole films, *Talanta* 78 (2009) 199–206.
- [37] I. Lähdesmäki, W.W. Kubiak, A. Lewenstam, A. Ivaska, Interferences in a polypyrrole-based amperometric ammonia sensor, *Talanta* 52 (2000) 269–275.
- [38] G. Anitha, E. Subramanian, Dopant induced specificity in sensor behavior of conducting polyaniline materials with organic solvents, *Sensors and Actuators B* 92 (2003) 49–59.
- [39] M. Penza, E. Milella, M.B. Alba, A. Quirini, L. Vasanelli, Selective NH<sub>3</sub> gas sensor based on Langmuir–Blodgett polypyrrole film, *Sensors and Actuators B* 40 (1997) 205–209.
- [40] H. Bai, Q. Chen, C. Li, C. Lu, G. Shi, Electrosynthesis of polypyrrole/sulfonated polyaniline composite films and their applications for ammonia gas sensing, *Polymer* 48 (2007) 4015–4040.
- [41] B. Timmer, W. Olthuis, A. Van den Berg, Ammonia sensors and their applications – a review, *Sensors and Actuators B* 107 (2005) 666–677.

## Biographies

**Tilia Patois** was born in 1986. She is a PhD student at the University of Franche-Comté, France. Her research consists in the development of gas sensors based on electrodeposited polymers.

**Jean-Baptiste Sanchez** received his PhD degree in chemical-physics from the University of Franche-Comté in 2005 where he is currently a lecturer. His current research interests are the development of a portable gas sensor for the sensitive and selective detection of pollutants in the atmosphere.

**Franck Berger** received his PhD degree in chemical-physics from the University of Franche-Comté in 1995. Since 1997, He is a teacher, researcher at the University of Franche-Comté. His research interests are the reaction mechanisms of the detection of various gases with tin dioxide gas sensors and the development of selective gas sensors.



**Jean-Yves Rauch** was born in 1969. He is currently working as Research Engineer in FEMTO-ST Institute (University of Franche-Comté). His scientific fields are every thin coating layers, vacuum technologies (PVD, CVD and PECVD) and surface analysis (XPS, XRD, and mass spectroscopy).

**Patrick Fievet** is full professor at the University of Franche-Comté, and Head of the “Nanoparticles, Contaminants, Membranes” group of the UTINAM Institute (UMR

CNRS 6213). His research interests include characterization and modeling of charge and transport properties of membranes.

**Boris Lakard** is full professor at the University of Franche-Comté, and member of the ‘Structured Materials and Surfaces’ group of the UTINAM Institute (UMR CNRS 6213). His research interests include electrodeposited polymers and their use in sensors and biosensors.